




## Article

# The Catalytic Upgrading Performance of NiSO<sub>4</sub> and FeSO<sub>4</sub> in the Case of Ashal'cha Heavy Oil Reservoir

Yasser I. I. Abdelsalam<sup>1</sup>, Leysan A. Akhmetzyanova<sup>2</sup>, Lilia Kh. Galiakhmetova<sup>1</sup>, Gadel F. Baimukhametov<sup>1</sup> , Rustam R. Davletshin<sup>1</sup>, Aleksey V. Dengaev<sup>3</sup>, Firdavs A. Aliev<sup>1,\*</sup>  and Alexey V. Vakhin<sup>1</sup> 

<sup>1</sup> Institute of Geology and Petroleum Technologies, Kazan Federal University, 18 Kremlyovskaya Str., Kazan 420008, Russia

<sup>2</sup> VNIIM-VNIIR, 7a 2nd Azinskaya Str., Kazan 420088, Russia

<sup>3</sup> Department of Petroleum Engineering, Gubkin National University of Oil and Gas, Leninskiy Prospect 65, Moscow 119991, Russia

\* Correspondence: aquathermolysis@gmail.com

**Abstract:** Aquathermolysis is a promising process for improving the quality of heavy oil under reservoir conditions. However, the application of catalysts during the process can significantly promote the transformation of the heavy fragments and heteroatom-containing compounds of crude oil mixtures into low-molecular-weight hydrocarbons. This research paper conducted a comparative analysis of the catalytic effectiveness of water-soluble metal salts like NiSO<sub>4</sub> and FeSO<sub>4</sub> in the process of aquathermolysis to upgrade heavy oil samples extracted from the Ashal'cha reservoir. The temperature of the experiment was 300 °C for a duration of 24 h. Compared to the viscosity of the native crude oil, the Fe nanoparticles contributed to a 60% reduction in viscosity. The viscosity alteration is explained by the chemical changes observed in the composition of heavy oil after catalytic (FeSO<sub>4</sub>) aquathermolysis, where the asphaltene and resin contents were altered by 7% and 17%, accordingly. Moreover, the observed aquathermolytic upgrading of heavy oil in the presence of FeSO<sub>4</sub> led to an increase in the yield of gasoline fraction by 13% and diesel fraction by 53%. The H/C ratio, which represents the hydrogenation of crude oil, increased from 1.52 (before catalytic upgrading) to 1.99 (after catalytic upgrading). The results of Chromatomass (GC MS) and Fourier-transform infrared spectroscopy (FT-IR) show the intensification of destructive hydrogenation reactions in the presence of water-soluble catalysts. According to the XRD and SEM-EDX results, the metal salts are thermally decomposed during the aquathermolysis process into the oxides of corresponding metals and are particularly sulfided by the sulfur-containing aquathermolysis products.

**Keywords:** catalytic hydrocracking; aquathermolysis; heavy oil; FeSO<sub>4</sub>; NiSO<sub>4</sub>; water-soluble catalysts; resins and asphaltenes; destructive hydrogenation; in situ upgrading



**Citation:** Abdelsalam, Y.I.I.; Akhmetzyanova, L.A.; Galiakhmetova, L.K.; Baimukhametov, G.F.; Davletshin, R.R.; Dengaev, A.V.; Aliev, F.A.; Vakhin, A.V. The Catalytic Upgrading Performance of NiSO<sub>4</sub> and FeSO<sub>4</sub> in the Case of Ashal'cha Heavy Oil Reservoir. *Processes* **2023**, *11*, 2426. <https://doi.org/10.3390/pr11082426>

Academic Editors: Jianhua Zhao, Guoheng Liu, Xiaolong Sun and Yuqi Wu

Received: 5 July 2023

Revised: 7 August 2023

Accepted: 8 August 2023

Published: 11 August 2023



**Copyright:** © 2023 by the authors. Licensee MDPI, Basel, Switzerland. This article is an open access article distributed under the terms and conditions of the Creative Commons Attribution (CC BY) license (<https://creativecommons.org/licenses/by/4.0/>).

## 1. Introduction

The prompt growth of population and extensive urbanization requires alternative energy resources to depleting conventional crude oil reserves in order to supply the energy demand. One of the alternative unconventional hydrocarbon resources is heavy oil. It is able to fill the gap in energy supply because of its abundant reserves worldwide and its sustainability. Generally, crude oils with a density of higher than 920 kg/m<sup>3</sup> and a viscosity of over 30 mPa·s are classified as heavy oils [1]. These types of hydrocarbons usually have a considerable proportion of large molecules, such as resins and asphaltenes [2–4]. Furthermore, these macromolecules also contain large quantities of sulfur, nitrogen, and oxygen compounds, which can lead to various challenges in the production, transportation, and processing of this type of crude oil [5–7]. In addition, the rich metal-containing complexes such as vanadyl and porphyrin, as well as other heavier metals in the structure of the heavy oils, are prone to poisoning the active catalysts used during crude oil processing in refineries. Due to the large macromolecules with high carbon content and relatively low

hydrogen ratio in comparison to conventional light crude oils, the production of value-added fractions is considerably lower [8,9]. Therefore, it is crucial to upgrade and improve the quality of such hydrocarbon resources before transferring them to refineries. Moreover, it is important to obtain high-quality or at least partially upgraded crude oil in reservoir formations in order to ease the mobility of crude oils through reservoir rocks and enhance the recovery efficiency.

Steam-based enhanced oil recovery methods currently continue to be the predominant techniques for effectively producing heavy oil and natural bitumen [10–12]. The structural traps with impermeable cap rocks that block the migration of the crude oil and lead to the accumulation of it can serve as natural reactors to carry out upgrading processes, where the heat is supplied by steam, hot water, etc. To date, many attempts have been made to upgrade heavy oil in situ by using steam under relatively mild conditions. This term was first introduced by Hyne et al. as “Aquathermolysis” [13–15]. However, the efficiency of aquathermolysis reactions was very low and was not sufficient for effective viscosity reduction, especially for heavy oils with high asphaltene content. Early in 1986, Hyne and his colleagues implied that some metal ions, i.e., nickel and cobalt, are believed to be involved in the cleavage of some bonds by hydrodesulfurization and hydrocracking processes, as well as water–gas shift reactions to produce hydrogen intermediates [16]. Since then, many authors have tried to design different types of catalysts, aiming to deliver them to oil reservoir formations, and transition metal-based catalysts have become of focal interest [17–22]. At present, the applied aquathermolysis catalysts can be divided into oil-soluble, water-soluble, and dispersed catalysts. Despite the efficiency of the latter catalysts, the injection of such catalysts by requiring stable suspension to the downhole is cost-effective and challenging. Instead, many authors are focused on developing oil-soluble catalysts based on different ligands due to the high sweep efficiency. Qin et al. synthesized oil-soluble iron oleate to improve aquathermolysis reactions [23]. The obtained laboratory data showed that the viscosity reduction degree was over 75% at 200 °C, 24 h, and a 0.3% catalyst solution concentration. The authors noted that the catalyst does not only promote the cleavage of C-S bonds but also accelerates the scission rate of C-O and C-N bonds [23]. Zhao et al. synthesized an oil-soluble catalyst based on a 2-ethyl-hexanoic acid ligand and evaluated its performance in upgrading heavy oil samples from the Liaohe field [24]. The content of light fractions increased, while the ratio of resins and asphaltenes decreased after the catalyst-assisted aquathermolytic upgrading. The authors reported a decrease in the content of sulfur by 0.5% and an increase in the atomic ratio of H/C from 1.63 to 2.0 [24]. Yi et al. carried out a comparison study to evaluate the efficiency of water-soluble catalysts and oil-soluble catalysts based on nickel (NiN) and iron naphthenates (FeN) on the aquathermolytic upgrading of resins and n-pentane asphaltenes, which were previously isolated from Liaohe heavy crude oil [25]. According to the authors, the activity sequence of the catalysts was as follows: without catalyst < NiSO<sub>4</sub> < FeSO<sub>4</sub> < NiN < FeN. This means that oil-soluble catalysts had higher efficiency than water-soluble ones in terms of the aquathermolytic upgrading of resins and asphaltenes. Al-Muntaser et al. [26] and [27] Suwaid et al. studied the role of oil-soluble catalysts based on metal stearate on the hydrogen donating capacity of decalin and improving the quality of heavy oil while utilizing conditions of steam injection. The authors imply that aquathermolytic upgrading using Ni stearate demonstrated catalytic activity in terms of hydrogen production and facilitating the in situ upgrading of hydrocarbons. Particularly, upgraded oil viscosity was reduced from 2034 mPa·s to 1031 mPa·s, measured in identical conditions. Moreover, a significant decrease was obtained in the resin and asphaltene contents of heavy oil from 26.30 and 8.26% to 16.55 and 1.49%, respectively. Some other organic ligands such as octanoate and decanoate are also reported as effective coupling compounds for the synthesis of oil-soluble aquathermolysis catalysts [7]. Although the oil-soluble catalyst precursors exhibited high catalytic performance in the aquathermolytic upgrading of heavy oil, the implementation of organometallic catalysts in the field can involve significant costs. The oil-soluble catalysts are expensive to obtain and require additional facilities for their

synthesis. The solubility of the catalyst precursors in organic solvents is also challenging, as not all the ligands can provide excellent solubility in the oil phase. This is crucial in terms of the injectivity and distribution of catalyst precursors through the porous reservoir rocks without precipitation. Moreover, the synthesis of oil-soluble catalysts has environmental challenges due to the additional applied chemicals and disposal of used water, which has to be treated or utilized. The management of any by-products generated during the synthesis may also pose challenges in terms of environmental impact. These procedures without any doubt significantly increase the cost of oil-soluble catalyst precursors.

On the other hand, water-soluble catalysts are known as cheap, easy-to-handle metal salts with less impact on the environment and pose minimal health and safety risks. Such catalyst precursors do not require other hazardous organic additives and do not require regeneration or separation from oil bulk. Meanwhile, water-soluble catalyst precursors can be directly injected into the well by dissolving salts in water to reduce the cost of implementation. The comparison of water-soluble and oil-soluble pre-catalysts is summarized in Table 1. Chen et al. synthesized a series of water-soluble metal complexes based on hydroxyl carbonyl acid and metal salts [28]. The authors evaluated the upgrading performance of the synthesized metal coordination complexes at 180 °C for 24 h for heavy crude oil with no sand from the Tazhong reservoir. Heavy oil sample viscosity was reduced by 80% using only 0.1% of the iron (III) coordination complex. Deng et al. developed a water-soluble catalytic complex based on Co (II) for the steam-based upgrading of heavy oil samples from the Huabei reservoir [29]. The introduction of 0.15% catalyst and 15% methanol to the aquathermolytic process carried out at 180 °C for 24 h resulted in a heavy oil viscosity reduction degree of 85.3%, and the pour point was altered by 9.0 °C. Clark et al. studied the influences of nickel and vanadyl salts, as well as transition metal cations on the aquathermolysis of sulfur-containing model compounds [15,30]. The authors found that certain cations were active for thiophane conversion, while others were reactive for tetrahydrothiophene, which was explained by the catalytic nature of the metals and the chemical properties of the model compounds. The same authors studied the catalytic efficiency of  $\text{Ru}^{2+}$ ,  $\text{Fe}^{2+}$ ,  $\text{Co}^{2+}$ ,  $\text{Os}^{3+}$ ,  $\text{Ir}^{3+}$ ,  $\text{Rh}^{3+}$ ,  $\text{Pd}^{2+}$ ,  $\text{Ni}^{2+}$ ,  $\text{Pt}^{2+}$ , and  $\text{Pt}^{4+}$  metal ions on the hydrodesulfurization of thiophene and tetrahydrothiophene during aquathermolysis processes [31]. The Pt (IV) solution revealed the best performance by reducing the content of sulfur at least by 40% (depending on the chemical nature of the used model compound). The iron (II) sulfate was used to promote the hydrocracking of bituminous oil at higher temperature ranges 375–415 °C [18]. This shows that the content of the asphaltenes in a crude oil mixture is not the sole deterministic factor of viscosity alteration. Zhong et al. investigated the synergetic effect of water-soluble Fe (II) and hydrogen donor solvent tetralin on the aquathermolytic upgrading of heavy oil samples from Liaohe [32]. The authors observed that with increasing Fe concentration, the viscosity of the heavy oil sample was further reduced. The hydrogen donor and iron catalyst without tetralin contributed to a viscosity reduction of 40% and 60%, respectively. Then, the combination of the water-soluble catalyst and hydrogen donor contributed to a viscosity decrease in the heavy oil sample by 90%. According to the temperature optimization study, the authors imply that the favorable temperature to carry out an aquathermolysis reaction is 240 °C. The research on exploring and developing new catalytic complexes is continued to better the efficiency of water-soluble catalysts. The stability and durability of the water-soluble catalysts are still poorly understood. Few researchers have addressed the problem of catalyst deactivation by the formation of coke-like substances under the harsh conditions of the aquathermolysis process. In this regard, developing water-soluble catalysts that can efficiently promote the aquathermolysis reactions, while suppressing unwanted side reactions and remaining active for a long period, is challenging. Further focus should be placed on the design of water-soluble catalysts, the optimization of operational conditions, and studying the overall mechanisms of heavy oil catalytic aquathermolysis. In the research [33], the authors used a graphene-supported bimetallic catalyst to enhance the viscosity reduction effect of heavy oil. The results showed that the viscosity reduction rate of heavy oil could reach 40–70%.

Table 1 summarizes the catalytic performance of water-soluble and oil-soluble pre-catalysts in terms of viscosity reduction degree during aquathermolysis of heavy oil.

**Table 1.** Oil-soluble and water-soluble catalysts.

	Catalyst	Reaction Conditions	Results of Upgrading Experiments	References
Oil-soluble catalysts.	Ni Co	180 °C	Viscosity reduced by 93.6%	[34]
	Nickel–molybdenum oleate	277 °C Nitrogen atmosphere	Viscosity reduction by 69%	[35]
	Iron sulfonate aroma	200 °C 6–7 MPa 24 h	Viscosity reduction by 90.7%	[36]
	Fe dodecylbenzene sulfonate	250 °C 24 h	Viscosity reduced by 79%	[37]
Water-soluble catalysts.	Ni	280 °C 8–10 MPa 24 h	Viscosity reduction by 87%	[38]
	Ru (III) chloride	415 °C 3 h	viscosity reduction by 98.6%	[39]
	Ni(CH <sub>3</sub> COO) <sub>2</sub>	300 °C 24 h	viscosity reduction by 58%	[40]

The aquathermolysis process involves the reaction of an aqueous solution of a metal sulfate, such as NiSO<sub>4</sub> or FeSO<sub>4</sub>, with heat to generate hydrogen gas. The mechanism of the catalytic aquathermolysis process includes several steps. The first is sulfate ion dissociation, which produces metal cations (Fe<sup>2+</sup> or Ni<sup>2+</sup>) and SO<sub>4</sub> anions. The released metal ions (Fe<sup>2+</sup> or Ni<sup>2+</sup>) adsorb onto the surface of the oil droplets present in the aquathermolysis process and after act as a catalyst, promoting the reaction between water (H<sub>2</sub>O) and the hydrocarbons present in the oil droplets. It is important to note that the aquathermolysis process is a complex reaction system influenced by various parameters, including temperature, pressure, feed composition, and catalyst concentration. The exact mechanism may vary depending on the specific conditions and feedstock being used.

The aim of the study is an evaluation of nickel and iron sulfates as water-soluble metal salts and their performance on the aquathermolytic upgrading of heavy oil from the Ashal'cha oil field at 300 °C for 24 h. We hope that our research will be beneficial for decision-makers in solving the problems regarding the application of water-soluble catalysts to enhance the production of heavy oil and upgrade it in situ.

## 2. Materials and Methods

Heavy oil samples produced from the Ashal'cha oil reservoir were the objects of research. The reservoir is located near Almet'yevsk, Russian Federation. The density and dynamic viscosity of the sample under normal conditions is 0.951 g/cm<sup>3</sup> and 3280 mPa·s, respectively. The average content of high-molecular components is about 45 %wt., and the content of sulfur can reach as high as 5 %wt.

The iron and nickel salts with an assay of more than 98%, which were manufactured for laboratory uses, were purchased from LLC «ChemTrade» (Russia Federation). The catalytic aquathermolysis processes with water-soluble catalysts NiSO<sub>4</sub> and FeSO<sub>4</sub> are conducted in a high-pressure and high-temperature batch reactor with a stirrer (HPHT), which is regulated by a control unit connected to a personnel computer for monitoring and recording the kinetics and the progress of the process. The HPHT reactor scheme is shown in Figure 1. The model system was initially purged with nitrogen for 20 min at room temperature to provide the inert ambiance of the process. Within 1 h after that,

the temperature in the reactor was increased up to 300 °C and kept for 24 h. The HPHT reactor was then cooled down to 25° C. Similar conditions were applied in our previous studies [40]. It allows us to simulate the extremal conditions of the steam-assisted enhanced oil recovery used in Russia [41]. The oil-to-water mass ratio of 70:30 was selected in order to simulate the process of aquathermolysis in steam-stimulated production techniques. The concentration of the catalyst was 2 %wt. from oil bulk.

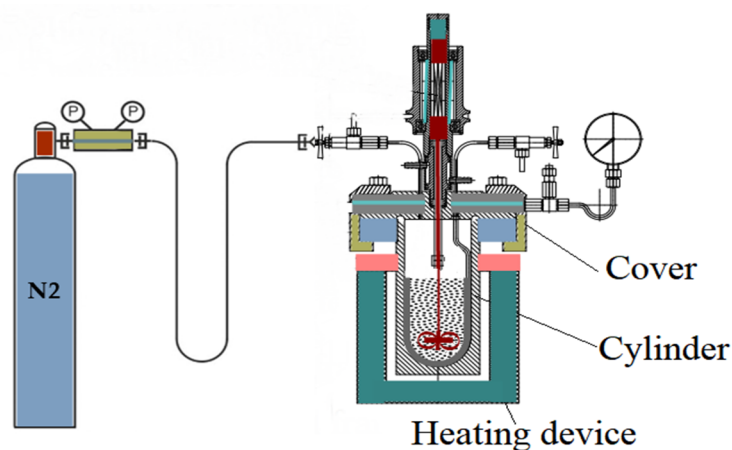


**Figure 1.** High-pressure and high-temperature reactor.

### 2.1. Elemental Analysis of Oil Samples

A Perkin Elmer 2400 Series II (Perkin Elmer, Waltham, MA, USA) Analyzer was used to evaluate the changes in the mass content of hydrogen, carbon, sulfur, and nitrogen in the composition of oil samples contributed by thermo-catalytic upgrading. The difference between the one and the sum of the CHNS content can be attributed to the content of oxygen. This method's results allow us to estimate the atomic ratio of H/C, which reflects the hydrogenation processes during aquathermolytic upgrading. Moreover, they provide information regarding the hydrodesulfurization, hydrodenitrogenation, and hydrodeoxygenation of oil.

### 2.2. FT-IR of Crude Oil Samples

For the Fourier-transform infrared spectroscopy analysis, a Vertex 70 FT-IR spectrometer (Bruker, Ettingen, Germany) was used. It allows us to identify the changes in the functional groups of samples under the influence of the catalytic systems. The infrared absorption characteristic peaks were analyzed in the wide range of 400–4000  $\text{cm}^{-1}$  wavenumbers.

### 2.3. Atmospheric Crude Distillation Unit

The crude oil atmospheric distillation was conducted in an ARN-LAB-03 distillation unit as per ASTM D86 [42]. The heavy oil samples were fractionated into light-end and heavy-end hydrocarbons. The light-end hydrocarbons referred to gasoline and diesel fractions with the boiling point ranges of the initial boiling point (i.b.p) at 200 °C and 200 °C–300 °C, respectively. The heavy-end hydrocarbons correspond to the fractions, the boiling points of which are higher than 300 °C.

### 2.4. Dynamic Viscosity of Crude Oil Samples

For the viscosity measurements, a Fungilab rotational viscometer Alpha L series combined with a temperature-maintaining unit MPC K6 from Huber (Offenburg, Germany) was used. The temperature-dependent viscosity values were measured at 20 °C, 40 °C, 60 °C, and 80 °C.

### 2.5. SARA-Analysis

The SARA analysis is a widely employed technique for characterizing different fractions of petroleum. It involves the chromatographic separation of crude oil into four primary categories based on polarity: saturates, aromatic compounds, resins, and asphaltenes. N-hexane was used to isolate maltenes from asphaltenes by adding it to the oil in a 1:40 oil-to-solvent ratio. In the given study, previously calcined aluminum oxides were used as the adsorbent in the chromatographic column. The chromatography column was tapped with a rubber tube after a portion of aluminum oxide was poured into the column for its sealing, and n-heptane was carefully poured into the upper part of the column. The n-heptane was passed through the column until the residue was discolored. The expiring fraction of saturates was collected. When the upper part of the aluminum oxide was almost dry, toluene was added to the column. The collecting flask was changed and the aromatics fraction was collected. The toluene was passed through until the expiring solvent was discolored. Then, a 150:50 toluene/methanol mixture was passed through the column in order to elute the resin fraction. The solvents of all three fractions were distilled and evaporated under a vacuum until a constant weight of fractions was reached.

### 2.6. Gas Chromatography-Mass Spectroscopy (GC MS)

The GC MS method was used to analyze the saturates and aromatics. The complex system was composed of a mass-selective detector ISQ produced in the USA and a gas chromatography “Chromatech-Crystal 5000” manufactured in Yoshkarala, Russia. The obtained results were processed using the XCalibur software. A capillary column with a length of 30 m and a diameter of 0.25 mm was employed. Helium was used as a carrier gas with a flowing rate of 1 mL/min, and the column temperature was set to 310 °C. The analysis started with a temperature increase from 100 °C to 150 °C at a heating rate of 3 °C/min, followed by a further increase to 300 °C in 8 min, and this temperature was maintained. In terms of the GC MS settings, the electron energy was set to 70 eV, and the ion source temperature was maintained at 250 °C. NIST Mass Spectral Library and relevant literature sources were used for the molecule and compound identification.

## 3. Results and Discussions

SARA analysis provides valuable information about the group composition of oil for the process evaluation. It allows us to understand the colloidal structure during different processes. The analysis also assists in predicting the stability of heavy oil and establishing the necessary measures to mitigate the challenges associated with heavy oil processing. The SARA fractions of initial (original) crude oil were compared with the fractions of non-catalytically upgraded oil samples (blank) and catalytically upgraded ones (Figure 2).

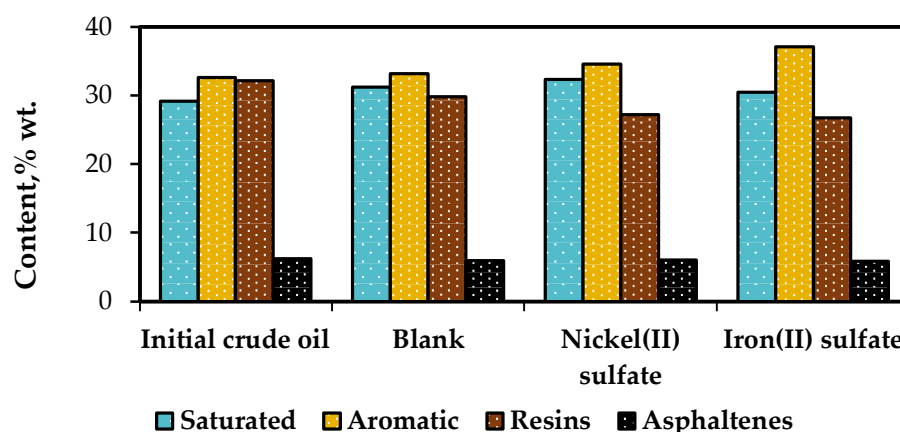


Figure 2. SARA analysis results for the samples.

Based on the data presented in Figure 2, the initial sample had a resin content of 32.1 %wt. and an asphaltene content of 6.2 %wt. Among the catalysts tested, iron (II) sulfate exhibited the most effective performance in enhancing the group composition. It led to a reduction in resin content by more than 16.8% compared to the initial sample. Additionally, the asphaltenes content decreased from 6.2 %wt. to 5.8 %wt. The presence of iron (II) sulfate facilitated the destructive hydrogenation of resins, which leads to an increase in saturate and aromatic contents from 29.1%wt. and 32.6%wt. to 30.4%wt. and 37.1%wt., respectively. On the other hand, nickel (II) sulfate similarly reduced resins content (27.2 %wt.), but the amount of asphaltenes remained similar to that of the blank sample (6 %wt.). These results show the influence of catalysts on aquathermolysis reactions leading to a reduction in heavy components and an increase in light components.

Viscosity is the most important technological property of oil, as it determines its mobility in the reservoir rock. The oil recovery factor strongly depends on the viscosity values. Some authors imply that viscosity depends on the content of asphaltenes [43,44]. In other words, the highly viscous crude oil contains a significant amount of asphaltenes. Thus, the viscosity increases due to the presence and size of macromolecular structures. A decrease in viscosity is expected with the destruction of primarily C-S bonds in heavy polar molecules and the hydrogenation of free radicals under aquathermolytic conditions.

Figure 3 shows the results of measuring the temperature-dependent viscosity characteristics of the initial oil and catalytic aquathermolysis products. The water-soluble catalysts  $\text{FeSO}_4$  and  $\text{NiSO}_4$  contributed an obvious viscosity reduction in samples in contrast to the blank and crude oil. The  $\text{FeSO}_4$  promoted the aquathermolytic scission of carbon-heteroatom bonds, which led to the viscosity decrease from 3250 mPa·s (initial crude oil) to 1306 mPa·s. Although the nickel (II) sulfate contributed to the viscosity alteration by 50%, the iron (II) sulfate performance was the highest at ~60%.

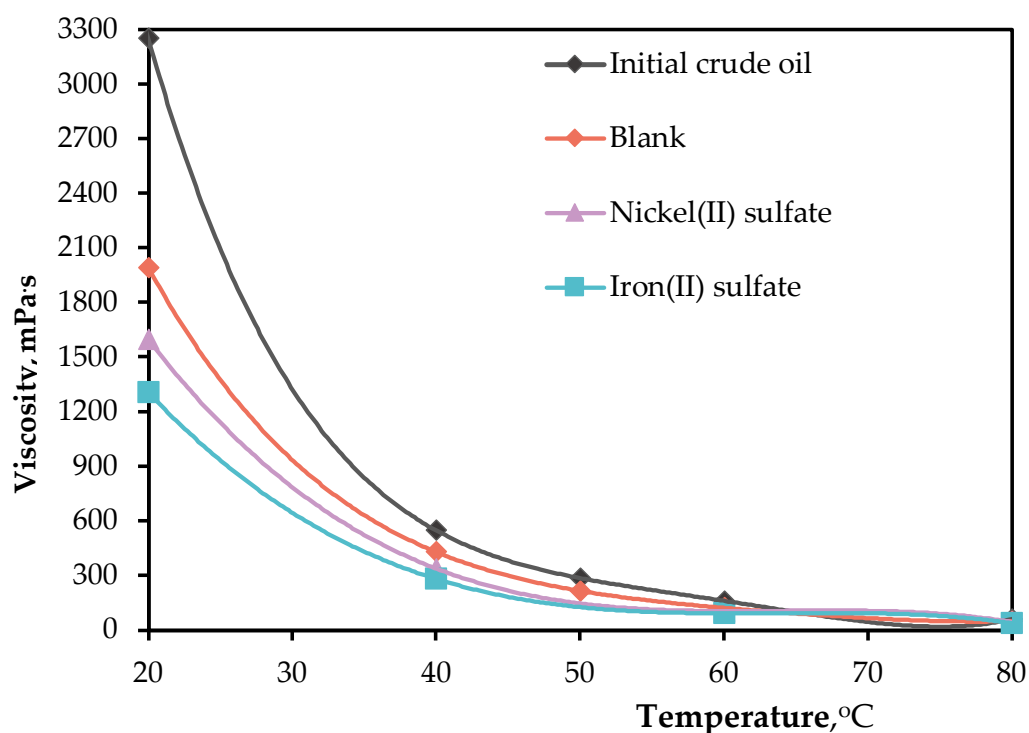


Figure 3. The viscosity of oil samples.

The high carbon and low hydrogen content of heavy oil determines the polyaromatic content, which determines its viscosity and quality. Upgrading heavy oil involves increasing the hydrogen content relative to carbon, thereby improving its quality owing to the hydrogenation reactions. Table 2 shows the atomic H/C ratio of oil samples before and after catalytic upgrading. Catalysts facilitated the hydrogenation reactions, wherein hydrogen was added to the heavy oil molecules, resulting in an increased H/C ratio.

**Table 2.** Effect of catalysts on the elemental analysis of oil samples.

Samples	Contents, %wt.				
	C	H	N	S	H/C <sub>atomic</sub>
Initial oil sample	83.34	10.63	0.48	5.55	1.52
Blank	81.80	13.52	0.00	4.68	1.98
NiSO <sub>4</sub>	81.90	13.57	0.00	4.53	1.99
FeSO <sub>4</sub>	81.83	13.59	0.00	4.57	1.99

The contribution of catalysts iron (II) sulfate and nickel (II) sulfate to the increase in the atomic ratio of H/C from 1.52 before the reaction to 1.99 indicates the formation of a significant number of aliphatic compounds after catalytic upgrading. In addition, water-soluble catalysts promoted the hydrodesulfurization of the heavy oil, which reduced the sulfur content from 5.5 %wt. to 4.5 %wt.

The atmospheric distillation of oil samples allows us to understand the effect of catalysts on the composition of the oil. The results of distillation are presented in Table 3.

**Table 3.** Atmospheric distillation of oil samples.

Samples	Initial Boiling Point Temperature, °C	Fraction Yield, %wt.				Total, % wt.
		Under 200 °C	200 °C–300 °C	Above 300 °C	Coke	
Initial oil sample	168	1.5	13.9	84.6		100
Blank	156	1.7	15.8	82.5	None	100
NiSO <sub>4</sub>	156	2.1	15.2	82.7	None	100
FeSO <sub>4</sub>	154	1.7	21.3	77.0	None	100

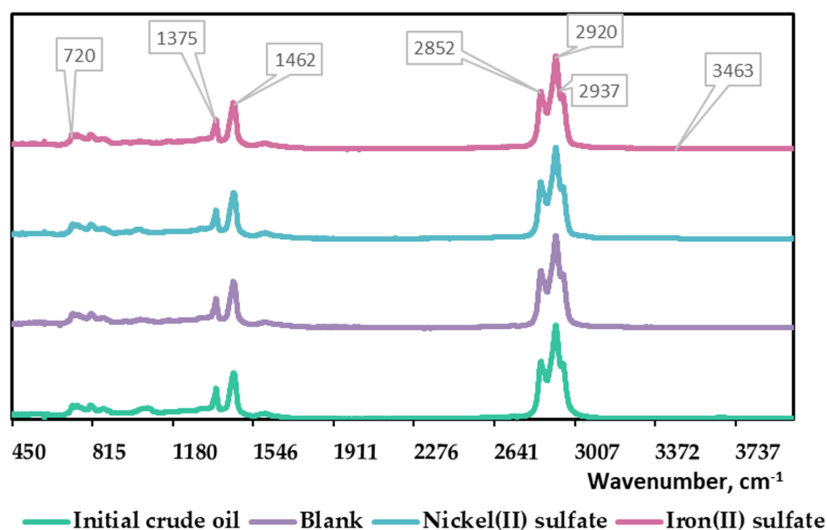
According to the results (Table 3), the initial boiling point for iron sulfate decreases from 168 °C to 154 °C, gasoline and diesel fractions increase by 13% and 53%, respectively, and fractions boiling above 300 °C are lower by 9% wt. The NiSO<sub>4</sub> catalyst contributes to an increase in gasoline and diesel fractions by 40% and 9%, respectively, and the fractions boiling above 300 °C are decreased by 2% wt.

FT-IR spectroscopy is used to assess alterations in the functional groups of oil samples. The obtained spectra (as shown in Figure 4) were analyzed to determine coefficients such as C1, aliphaticity; C2, aromaticity; C3, branching; C4, condensation; C5, oxidation; and C6 and C7, sulfurization degrees. These coefficients were estimated according to reference [45] and are summarized in Table 4.

**Table 4.** Spectral coefficients of oil samples based on FTIR spectra.

	C1	C2	C3	C4	C5	C6	C7
Crude oil	8.5	0.5	1.9	0.4	0.3	1.9	1.3
Blank	7.2	0.5	1.8	0.5	0.5	1.4	1.2
NiSO <sub>4</sub>	7.4	0.5	1.7	0.5	0.4	1.6	1.3
FeSO <sub>4</sub>	6.9	0.5	1.8	0.5	0.3	1.3	1.3





Wavenumbers, cm <sup>-1</sup>	Peaks and the vibration forms of infrared absorption characteristics
3500–3300	-NH <sub>2</sub> or free -NH, stretching vibration
2933–2923, 2860–2840	-CH <sub>2</sub> , symmetric and antisymmetric vibrations (Rej et al., 2022)
1680–1620	C=C, stretching vibration
1850–1600	-C=O (alcohols, aldehydes, acids, ketones, etc.), stretching vibration
1470–1450	-CH <sub>3</sub> , -CH <sub>2</sub> , deformation vibration
1608, 1460	Asymmetric stretching vibration of framework phenyl rings C=C
1380–1370	-CH <sub>3</sub> , symmetrical deformation vibration
1300–1000	C-O, stretching vibration (Rej et al., 2022)
733–723	-(CH <sub>2</sub> ) <sub>n</sub> , n C 4
800–600	C-Cl

**Figure 4.** FTIR spectra of crude oil samples [46].

The spectral coefficient calculation methods are aliphaticity (C1)—this coefficient represents the ratio of the intensity at 1450 cm<sup>-1</sup> (D1450) to the intensity at 1600 cm<sup>-1</sup> (D1600) and indicates the proportion of C-H and C=C bonds of aliphatic and aromatic structures, respectively; aromaticity (C2)—this coefficient represents the ratio of the intensity at 1600 cm<sup>-1</sup> (D1600) to the sum of the intensities at 720 cm<sup>-1</sup> and 1380 cm<sup>-1</sup> (D720 + 1380) and indicates the proportion of C=C bonds and C-H bonds; branching (C3)—this coefficient represents the ratio of the intensity at 1380 cm<sup>-1</sup> (D1380) to the intensity at 720 cm<sup>-1</sup> (D720) and indicates the proportion of methylene groups to methyl groups; degree of condensation (C4)—this coefficient represents the ratio of the intensity at 1600 cm<sup>-1</sup> (D1600) to the sum of the intensities at 740 cm<sup>-1</sup> and 860 cm<sup>-1</sup> (D740 + 860) and shows the proportion of C=C bonds in aromatic groups compared to C-H bonds in aromatic structures and provides information about the degree of condensation; degree of oxidation (C5)—this coefficient represents the ratio of the intensity at 1700 cm<sup>-1</sup> (D1700) to the intensity at 1600 cm<sup>-1</sup> (D1600) and indicates the proportion of carbonyl groups R-C=O (in the presence of an OH-group) compared to C=C bonds in aromatic structures, providing insight into the degree of oxidation; degree of sulfurization (C6)—this coefficient represents the ratio of the intensity at 1030 cm<sup>-1</sup> (D1030) to the intensity at 1600 cm<sup>-1</sup> (D1600) and shows the proportion of S=O bonds in sulfoxide groups (either in sulfonates or sulfonic acids, provided that the absorption bands are in the range of 1260–1150 cm<sup>-1</sup> and 700–600 cm<sup>-1</sup>) compared to C=C bonds in aromatic groups, indicating the degree of sulfurization; degree of sulfurization (C7)—this coefficient represents the ratio of the intensity at 1160 cm<sup>-1</sup> (D1160) to the intensity at 1600 cm<sup>-1</sup> (D1600) and shows the proportion of S=O bonds in sulfonate groups compared to C=C bonds in aromatic groups, providing information about the degree of sulfurization. These coefficients were calculated to evaluate various chemical

characteristics of the analyzed samples based on their infrared spectra. They provide valuable information about the aliphaticity, aromaticity, branching, degree of condensation, degree of oxidation, and degree of sulfurization in the studied compounds.

According to Table 4, the coefficients of aliphaticity (C1), branching (C3), and sulfurization (C6) are decreased. At the same time, there is an increase in the condensation (C4) and oxidation (C5) coefficients. These changes strongly suggest that there is a compaction of the naphthenic molecule, along with the substitution of alkyl-naphthene fragments with functional groups containing sulfur and oxygen.

Figure 5 shows the results of the GC MS analysis of saturated hydrocarbons separated from the oil samples. According to analysis, changes are observed in the lower retention time zone corresponding to the high-molecular-weight n-alkanes. Particularly, the number of normal alkanes with carbon chain lengths longer than 21 in the composition of saturates separated from the oil sample upgraded in the presence of iron sulfate is almost twice the intensity of the corresponding peak observed in the saturate fraction of the blank sample. However, the number of iso-alkanes upgraded using iron sulfate is less than the normal alkanes of the blank sample. According to the spectra, the peaks corresponding to hopanes and homohopanes are also intensified in the presence of both water-soluble metal salts.

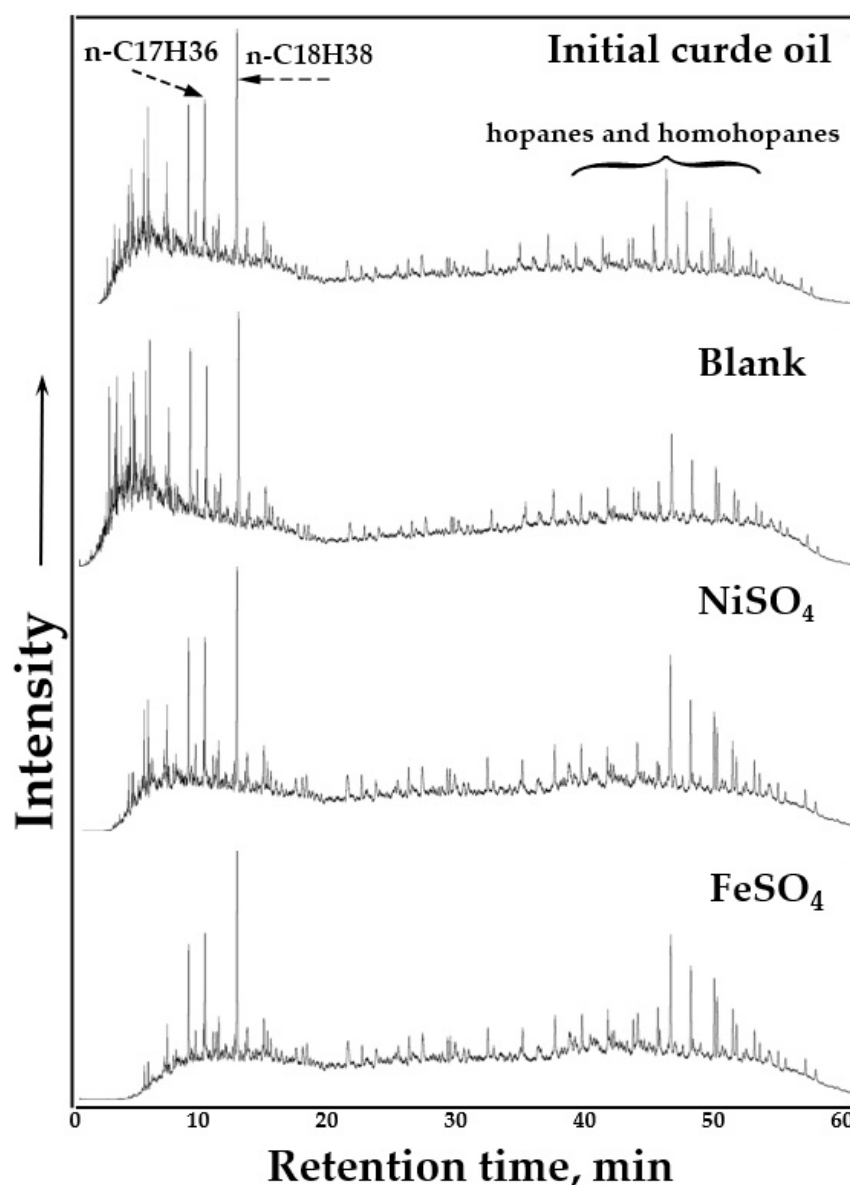


Figure 5. The mass spectra of saturates as per TIC.

The relative content of iso-alkanes separated from the samples and normal alkanes with a carbon chain of less than 20 and more than 21 are presented in Figure 6. The relative quantitative analysis was employed based on the comparison of the spectral area behind the peaks of the samples and the results of the relative content of normal alkanes with carbon chains of fewer than 20 and more than 21. The nickel (II) sulfate led to the change in low-molecular-weight normal alkanes from 8 to 10%; at the same time, for iron (II) sulfate, the number of C10–C20 n-alkanes was unchanged (8%). However, iron sulfate significantly increased the content of normal alkanes with high molecular weight by more than 60% compared to the blank sample. Moreover, the given catalyst contributed to altering the number of iso-alkanes from 72% to 66%.

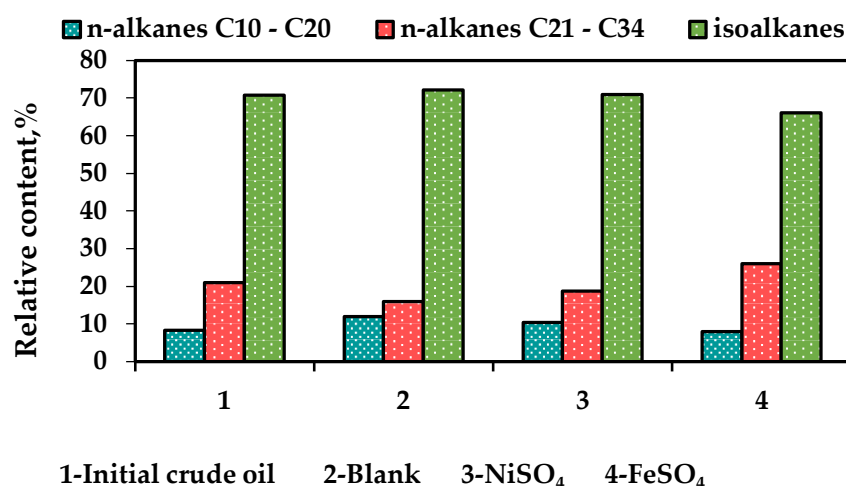


Figure 6. Content of normal alkanes and iso alkanes in the samples.

Figure 7 shows the comparison between the relative number of saturated hydrocarbons (alkanes) and other compounds such as alkenes and hopanes. The study found that for the blank oil samples, the percentage of alkanes changed from 61% to 52%, while the proportion of cyclic hydrocarbons almost doubled. However, the addition of the nickel (II) and iron (II) sulfates to the system contributed to the decrease in the number of cyclic compounds from 30% (blank sample) to 9% and 6%, accordingly. On the other hand, the number of hopanes was increased twice in the presence of both water-soluble catalysts.

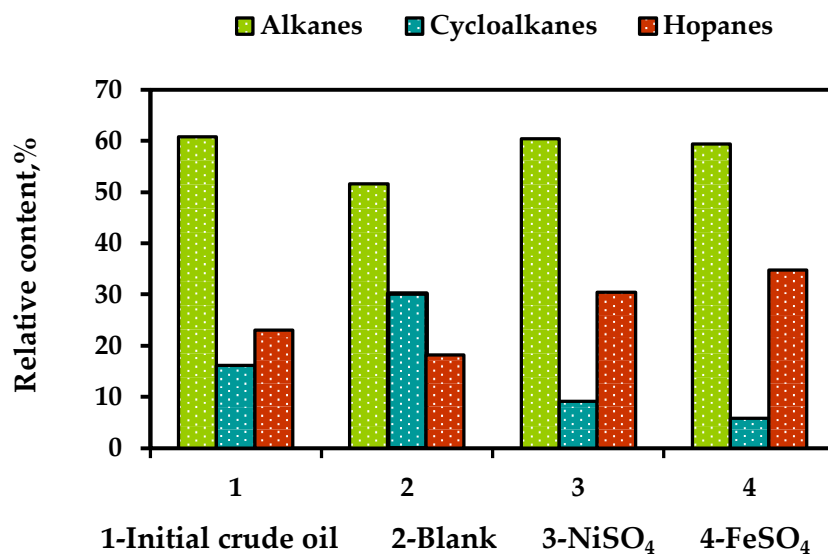


Figure 7. Relative content of saturated hydrocarbons for the samples.

Figure 8 shows the recorded aromatic hydrocarbons in the mode of TIC mass spectra. According to the spectra, significant changes were observed in the intensity of alkyl benzenes and thiophenes peaks. The intensity of C<sub>18</sub>H<sub>30</sub> and heavier aromatic rings peaks with a retention time of 22 min and higher are significantly reduced with the addition of the water-soluble catalysts. The results of a quantitative analysis of aromatic hydrocarbon compounds are illustrated in Figure 9. The proportion of alkylbenzenes decreased from 29% to 24% for the blank samples. The reduction in alkylbenzenes content with catalysts was 16%. The naphthalene content in the aromatic fraction after catalytic treatment increased from 9% to 11% compared to blank samples. This suggests that the presence of catalysts had an impact on the distribution of naphthalene. After both the catalytic and non-catalytic processes, the content of biphenyls and other compounds slightly increased. This demonstrates the detachment of peripheral radicals from condensed aromatic rings of resins and asphaltenes, which were bonded by means of C-N, C-S, and C-O bonding and further joined the aromatic hydrocarbons.

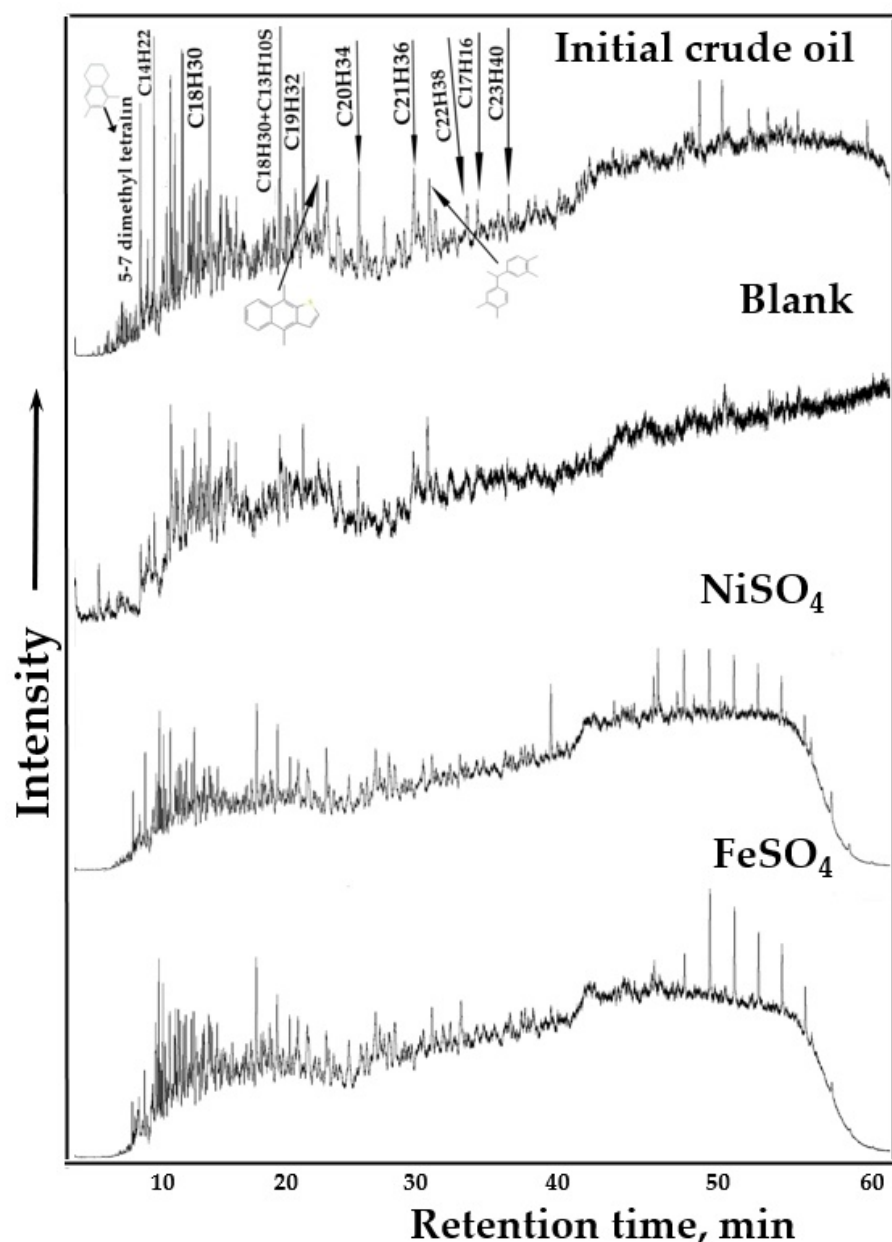


Figure 8. The mass spectra of aromatics.

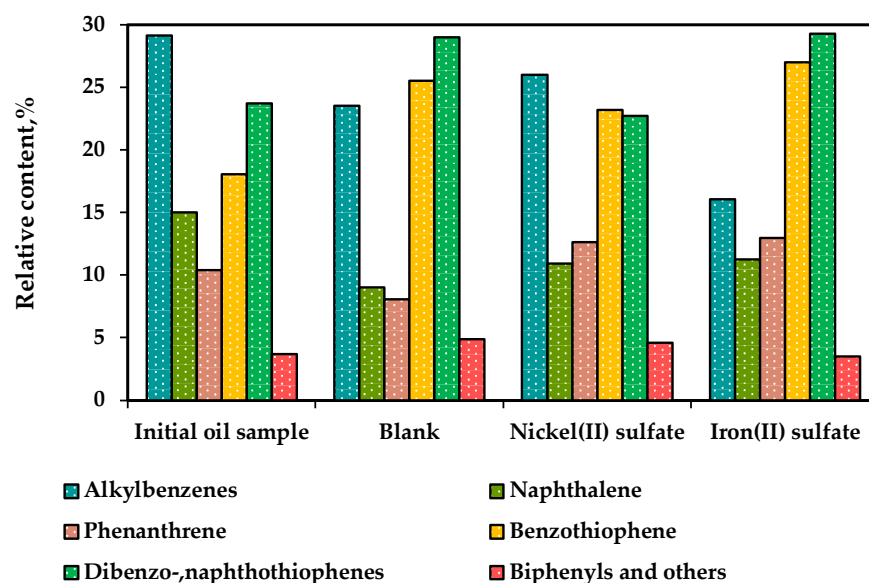


Figure 9. The content fraction of aromatic compounds.

The nature of the microstructure can be seen over a wide magnification range of the Scanning Electron Microscopy (SEM) analysis method. In general, SEM analysis is used to facilitate the comparison and explanation of microstructures. In SEM images, the microscope is used to qualitatively determine microstructural changes in the matrix of catalyst samples (Figures 10–12). In this way, the microstructure is easy to observe because the images can be magnified. The structure of the catalyst samples was imaged after the aquathermolysis processes. The data obtained by EDX provide information on the elemental composition of the metals formed in the reaction as well as the end of the process. Both large-scale and individual surface analyses were performed. The average metal oxide and sulfide particle sizes were identified in a micron range. According to the elemental composition (Figure 11), the share of nickel oxides prevails in its sulfide form as the content of oxygen—48 %wt.—while sulfur is only 10 %wt. The high ratio of carbon (21 %wt., Figure 11) indicates the adsorption of heavy oil high molecular-weight fragments, which are not dissolved in organic solvents such as carbenes and carboids on the surface of the nickel catalyst particles. At the same time, the sulfur content is relatively higher (18%wt., Figure 12) in the composition of the iron-based catalyst surface. This indicates that iron (II) sulfate is prone to sulfidation by hydrogen sulfide and other sulfur-containing by-products of the aquathermolysis process. Moreover, according to the content of carbon (10 %wt., Figure 12), iron oxides and sulfides contribute less to coke formation. Hence, such catalysts can withstand the reservoir formation coking process for longer and remain active.

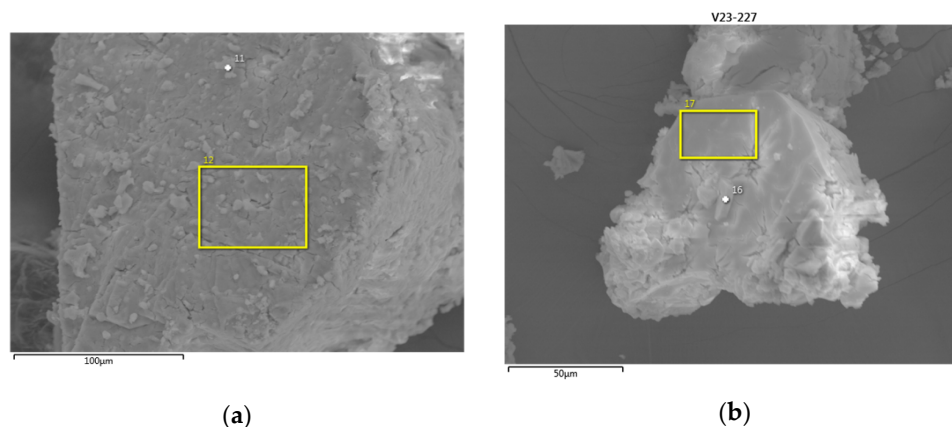


Figure 10. SEM analysis of (a)  $\text{NiSO}_4$  and (b)  $\text{FeSO}_4$  after the aquathermolysis process.

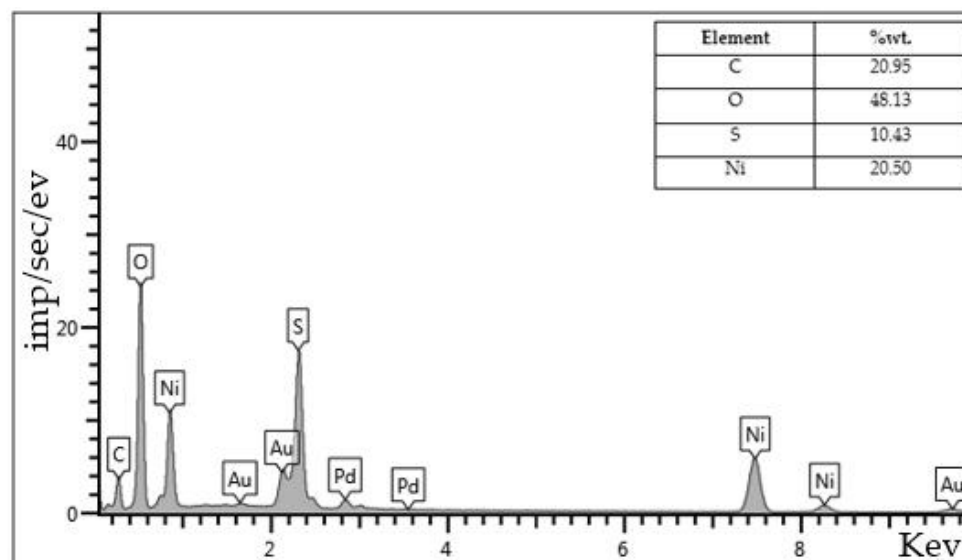


Figure 11. The EDX of the  $\text{NiSO}_4$  isolated from upgraded oil bulk.

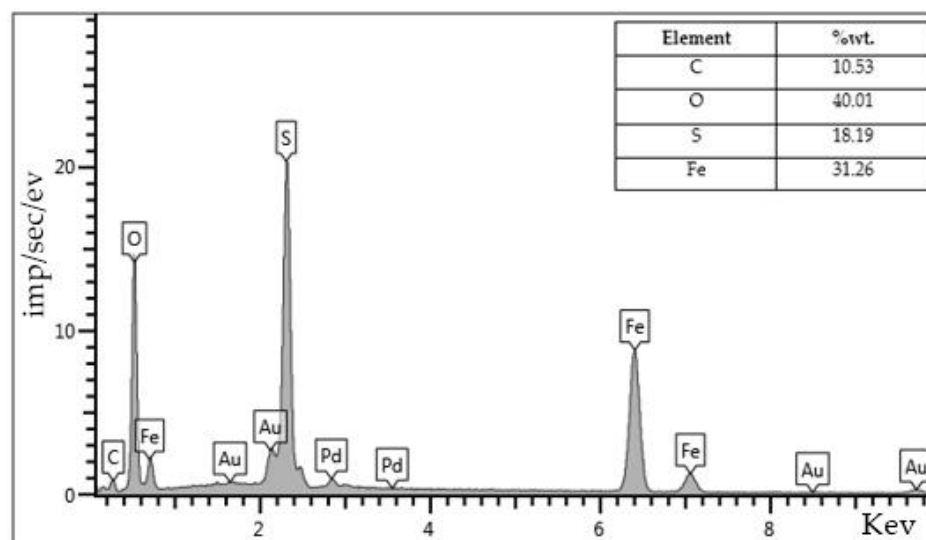
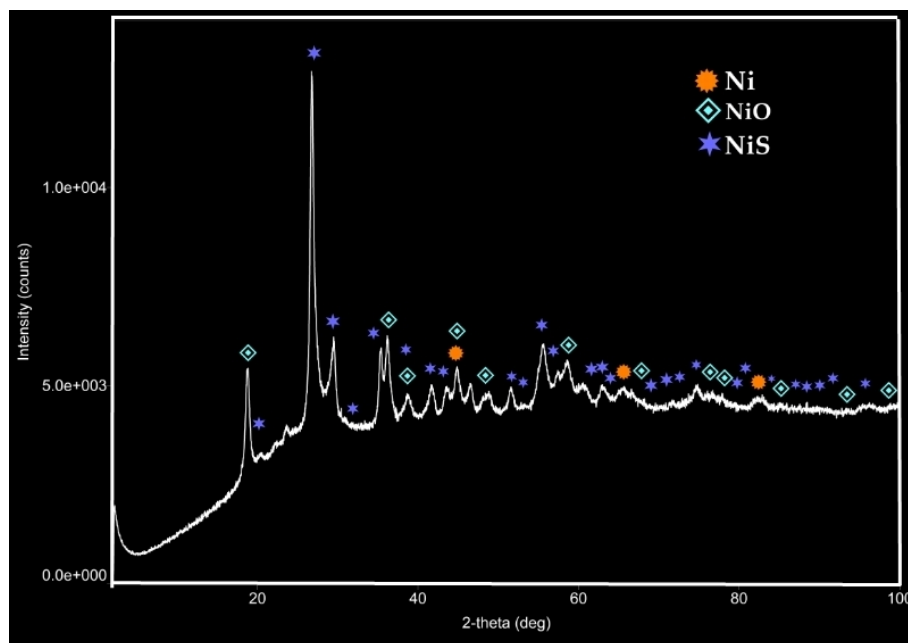
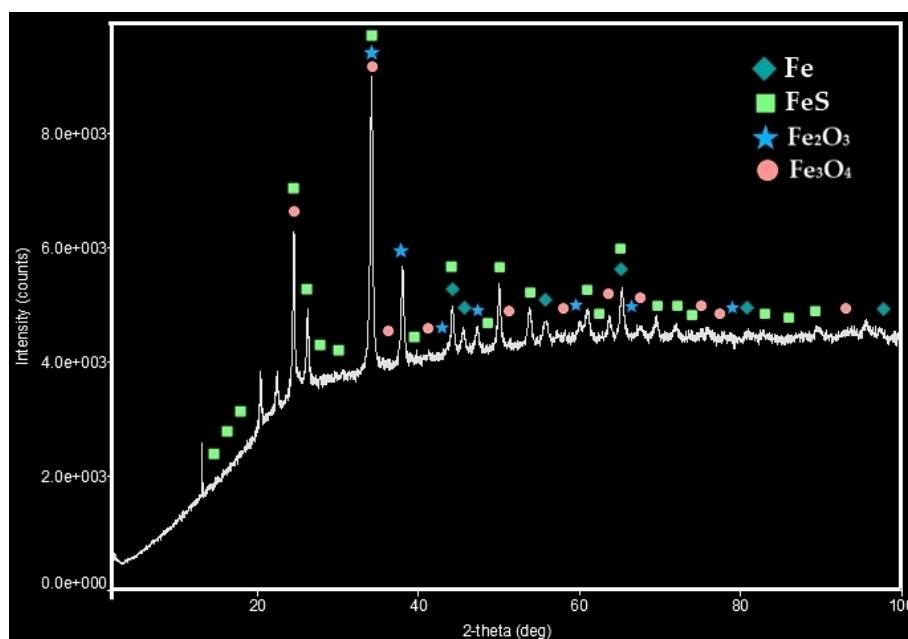


Figure 12. The EDX of the  $\text{FeSO}_4$  isolated from upgraded oil bulk.

In conjunction with the SEM-EDX analysis method, XRD patterns of the isolated catalyst particles from oil bulk after the aquathermolysis process (Figures 13 and 14) provide further characterization of the morphology, phase composition, and crystalline structure of the metal sulfates' thermal decomposition products. The patterns are characterized by a series of sharp peaks corresponding to the crystal lattice planes of Ni JCPDS (01-080-5763), NiO JCPDS (01-085-1977), and NiS JCPDS (01-079-9975) in the case of nickel (II) sulfate and Fe JCPDS (01-080-3818), FeS JCPDS (00-029-0723), hematite ( $\text{Fe}_2\text{O}_3$ ) JCPDS (01-080-5407), and magnetite ( $\text{Fe}_3\text{O}_4$ ) JCPDS (00-028-0491) in case of iron (II) sulfate. Nickel oxide is a cubic crystal structure with a characteristic peak at  $2\theta$  values of approximately  $19.8^\circ$ ,  $37.5^\circ$ ,  $42.5^\circ$ ,  $58^\circ$  and  $79^\circ$ . Nickel sulfide, or by another name, millerite, has a hexagonal crystal structure. Its XRD pattern shows peaks at  $2\theta$  values of approximately  $20.9^\circ$ ,  $27^\circ$ ,  $42.6^\circ$ ,  $54.9^\circ$ ,  $62.7^\circ$ , and  $69.4^\circ$ . The intensity of the XRD pattern of the nickel phase is relatively very low and presented by  $2\theta$  values of  $43^\circ$  and  $66^\circ$ .



**Figure 13.** XRD patterns of nickel (II) sulfate isolated from crude oil after the aquathermolysis process.



**Figure 14.** XRD patterns of iron (II) sulfate isolated from crude oil after the aquathermolysis process.

The thermal decomposition products of iron (II) sulfate in aquathermolytic conditions are primarily presented by pyrrhotite (FeS), which indicates the involvement of the sulfur-containing by-products of the aquathermolysis reactions in the sulfidation of the metal oxides. The prominent peaks around  $2\theta$  were observed in the XRD pattern of FeS:  $23.9^\circ$ ,  $42^\circ$ ,  $50^\circ$ ,  $55^\circ$ ,  $63.8^\circ$ ,  $71.9^\circ$ . Hematite and magnetite have rhombohedral and cubic crystal structures, accordingly.

#### 4. Conclusions

This study was devoted to the catalytic performance of water-soluble catalysts  $\text{NiSO}_4$  and  $\text{FeSO}_4$  for upgrading heavy oil by means of an aquathermolysis process in situ. The obtained experimental data revealed that the catalysts contributed to the intensification

of the C-S and C=C bonds scission, which led to the light components increasing while significantly reducing the heavy components. At the same time, the upgraded oil was further diluted with light hydrocarbons, which led to a viscosity reduction. Among both catalysts used, the FeSO<sub>4</sub> catalyst demonstrated the highest degree of viscosity reduction, reaching 60%. The composition of the hydrocarbons significantly changed during the iron (II) sulfate-assisted aquathermolytic upgrading. The content of saturates and aromatics increased from 29.1% and 32.6% to 36.3% and 40.2%, respectively. In contrast, the content of resins decreased by 17%, while the amount of asphaltenes decreased by 12.9%. The initial boiling point of catalyst-assisted upgraded oil decreased from 168 °C to 154 °C and also led to the gasoline and diesel fractions increasing by 13% and 53%, respectively. The NiSO<sub>4</sub> catalyst led to an increase in gasoline and diesel fractions by 40% and 9%, respectively. The IR spectra showed that hydrogenation and heteroatom removal reactions took place during the catalytic aquathermolysis process, leading to a decrease in the aliphaticity, branching, and sulfurization spectral coefficients, while the condensation and oxidation coefficients were increased. The thermal decomposition products of metal salts were identified by SEM-EDX and XRD as the oxides and sulfides of the corresponding metals. The obtained results allow us to extend catalysts' use in the aquathermolysis process. At the same time, the introduced method can be as effective as previous methods; however, it brings wider opportunities for catalysts' use in the aquathermolysis process.

**Author Contributions:** Conceptualization, F.A.A.; Methodology, F.A.A.; Investigation, Y.I.I.A. and L.K.G.; Resources, L.A.A., A.V.D. and A.V.V.; Data curation, Y.I.I.A. and R.R.D.; Writing—original draft, F.A.A.; Writing—review & editing, Y.I.I.A. and G.F.B.; Supervision, F.A.A. and A.V.V.; Funding acquisition, A.V.V. All authors have read and agreed to the published version of the manuscript.

**Funding:** This work was supported by the Russian Science Foundation (Grant No. 21-73-30023).

**Data Availability Statement:** Data available on request.

**Conflicts of Interest:** The authors declare no conflict of interest.

## References

1. Meyer, R.F.; Attanasi, E.D.; Freeman, P.A. Heavy Oil and Natural Bitumen Resources in Geological Basins of the World. Open File-Report 2007–1084. *Usgs* **2007**, *140*, 198–203. [[CrossRef](#)]
2. Vakhin, A.V.; Aliev, F.A.; Mukhamatdinov, I.I.; Sitnov, S.A.; Sharifullin, A.V.; Kudryashov, S.I.; Afanasiev, I.S.; Petrashov, O.V.; Nurgaliev, D.K. Catalytic Aquathermolysis of Boca de Jaruco Heavy Oil with Nickel-Based Oil-Soluble Catalyst. *Processes* **2020**, *8*, 532. [[CrossRef](#)]
3. Vakhin, A.V.; Mukhamatdinov, I.I.; Aliev, F.A.; Feoktistov, D.F.; Sitnov, S.A.; Gafurov, M.R.; Minkhanov, I.F.; Varfolomeev, M.A.; Nurgaliev, D.K.; Simakov, I.O. Industrial Application of Nickel Tallate Catalyst during Cyclic Steam Stimulation in Boca De Jaruco Reservoir. In Proceedings of the SPE Russian Petroleum Technology Conference, OnePetro, Virtual, 12–15 October 2021.
4. Dong, X.; Liu, H.; Chen, Z.; Wu, K.; Lu, N.; Zhang, Q. Enhanced Oil Recovery Techniques for Heavy Oil and Oilsands Reservoirs after Steam Injection. *Appl. Energy* **2019**, *239*, 1190–1211. [[CrossRef](#)]
5. Aliev, F.; Kholmurodov, T.; Mirzayev, O.; Tajik, A.; Mukhamadiev, N.; Slavkina, O.; Nourgalieva, N.; Vakhin, A. Enhanced Oil Recovery by In-Reservoir Hydrogenation of Carbon Dioxide Using Na-Fe<sub>3</sub>O<sub>4</sub>. *Catalysts* **2023**, *13*, 153. [[CrossRef](#)]
6. Abdelsalam, Y.I.I.; Khamidullin, R.F.; Katnov, V.E.; Dengaev, A.V.; Aliev, F.A.; Vakhin, A.V. Influence of FeP and Al(H<sub>2</sub>PO<sub>4</sub>)<sub>3</sub> Nanocatalysts on the Thermolysis of Heavy Oil in N<sub>2</sub> Medium. *Catalysts* **2023**, *13*, 390. [[CrossRef](#)]
7. Tirado, A.; Félix, G.; Suwaid, M.A.; Al-Muntaser, A.A.; Antonenko, D.A.; Afanasiev, I.S.; Varfolomeev, M.A.; Yuan, C.; Ancheyta, J. Modeling the Kinetics of Heavy Crude Oil Cu-Oleate Aquathermolysis. *Ind. Eng. Chem. Res.* **2023**, *62*, 9114–9122. [[CrossRef](#)]
8. Dorner, R.W.; Hardy, D.R.; Williams, F.W.; Willauer, H.D. Heterogeneous Catalytic CO<sub>2</sub> Conversion to Value-Added Hydrocarbons. *Energy Environ. Sci.* **2010**, *3*, 884–890. [[CrossRef](#)]
9. Aliev, F.; Mirzaev, O.; Kholmurodov, T.; Slavkina, O.; Vakhin, A. Utilization of Carbon Dioxide via Catalytic Hydrogenation Processes during Steam-Based Enhanced Oil Recovery. *Processes* **2022**, *10*, 2306. [[CrossRef](#)]
10. Hart, A. Advanced Studies of Catalytic Upgrading of Heavy Oils 2014. Available online: <https://etheses.bham.ac.uk/id/eprint/5297/2/Hart14PhD.pdf> (accessed on 1 June 2023).
11. Yuan, C.; Varfolomeev, M.A.; Kok, M.V.; Nurgaliev, D.K.; Gabbasov, A.H. Applications of Enhanced Oil Recovery Techniques of Heavy Crudes. In *Catalytic In-Situ Upgrading of Heavy and Extra-Heavy Crude Oils*; Wiley: Hoboken, NJ, USA, 2023; pp. 153–167.
12. Vakhin, A.; Aliev, F.; Kaukova, G.; Al-Muntaser, A.A.; Suwaid, M.A.; Yuan, C.; Ancheyta, J.; Varfolomeev, M.A. Fundamentals of In Situ Upgrading. In *Catalytic In-Situ Upgrading of Heavy and Extra-Heavy Crude Oils*; Wiley: Hoboken, NJ, USA, 2023; pp. 168–236.



13. Hyne, J.B.; Greidanus, J.W.; Tyrer, J.D.; Verona, D.; Clark, P.D.; Clarke, R.A.; Koo, J.H.F. «The Future of Heavy Crude and Tar Sands» Aquathermolysis of heavy oils. In Proceedings of the 2nd International Conference, Caracas, Venezuela, 7–17 February 1982; pp. 404–411.
14. Hyne, J.B.; Clark, P.D.; Clarke, R.A.; Koo, J.; Greidanus, J.W. Aquathermolysis of Heavy Oils. *Rev. Tec. Intevep*. **1982**, *2*, 87–94.
15. Clark, P.D.; Hyne, J.B. Chemistry of Organosulphur Compound Types Occurring in Heavy Oil Sands: 3. Reaction of Thiophene and Tetrahydrothiophene with Vanadyl and Nickel Salts. *Fuel* **1984**, *63*, 1649–1654. [[CrossRef](#)]
16. Hyne, J.B. Aquathermolysis: A Synopsis of Work on the Chemical Reaction between Water (Steam) and Heavy Oil Sands during Simulated Steam Stimulation. *AOSTRA Publ. Ser.* **1986**, *55*, 110.
17. Clark, P.D.; Clarke, R.A.; Hyne, J.B.; Lesage, K.L. Studies on the Effect of Metal Species on Oil Sands Undergoing Steam Treatments. *Aostr J. Res.* **1990**, *6*, 53–64.
18. Clark, P.D.; Kirk, M.J. Studies on the Upgrading of Bituminous Oils with Water and Transition Metal Catalysts. *Energy Fuels* **1994**, *8*, 380–387. [[CrossRef](#)]
19. Clark, P.D.; Hyne, J.B. Studies on the Chemical Reactions of Heavy Oils under Steam Stimulation Condition. *Aostr J. Res.* **1990**, *29*, 29–39.
20. Quitian, A.; Fernández, Y.; Ancheyta, J. Viscosity Reduction of Heavy Oil during Slurry-Phase Hydrocracking. *Chem. Eng. Technol.* **2019**, *42*, 148–155. [[CrossRef](#)]
21. Maity, S.K.; Ancheyta, J.; Marroquín, G. Catalytic Aquathermolysis Used for Viscosity Reduction of Heavy Crude Oils: A Review. *Energy Fuels* **2010**, *24*, 2809–2816. [[CrossRef](#)]
22. Maity, S.K.; Ancheyta, J.; Alonso, F.; Rayo, P. Hydrodesulfurization Activity of Used Hydrotreating Catalysts. *Fuel Process. Technol.* **2013**, *106*, 453–459. [[CrossRef](#)]
23. Qin, W.L.; Xiao, Z.L. The Researches on Upgrading of Heavy Crude Oil by Catalytic Aquathermolysis Treatment Using a New Oil-Soluble Catalyst. *Adv. Mater. Res.* **2013**, *608–609*, 1428–1432. [[CrossRef](#)]
24. Zhao, F.; Liu, Y.; Fu, Z.; Zhao, X. Using Hydrogen Donor with Oil-Soluble Catalysts for Upgrading Heavy Oil. *Russ. J. Appl. Chem.* **2014**, *87*, 1498–1506. [[CrossRef](#)]
25. Yi, Y.; Li, S.; Ding, F.; Yu, H. Change of Asphaltene and Resin Properties after Catalytic Aquathermolysis. *Pet. Sci.* **2009**, *6*, 194–200. [[CrossRef](#)]
26. Al-Muntaser, A.A.; Varfolomeev, M.A.; Suwaid, M.A.; Saleh, M.M.; Djimasbe, R.; Yuan, C.; Zairov, R.R.; Ancheyta, J. Effect of Decalin as Hydrogen-Donor for in-Situ Upgrading of Heavy Crude Oil in Presence of Nickel-Based Catalyst. *Fuel* **2022**, *313*, 122652. [[CrossRef](#)]
27. Suwaid, M.A.; Varfolomeev, M.A.; Al-muntaser, A.A.; Yuan, C.; Starshinova, V.L.; Zinnatullin, A.; Vagizov, F.G.; Rakhmatullin, I.Z.; Emelianov, D.A.; Chemodanov, A.E. In-Situ Catalytic Upgrading of Heavy Oil Using Oil-Soluble Transition Metal-Based Catalysts. *Fuel* **2020**, *281*, 118753. [[CrossRef](#)]
28. Chen, G.; Yan, J.; Bai, Y.; Gu, X.; Zhang, J.; Li, Y.; Jeje, A. Clean Aquathermolysis of Heavy Oil Catalyzed by Fe (III) Complex at Relatively Low Temperature. *Pet. Sci. Technol.* **2017**, *35*, 113–119. [[CrossRef](#)]
29. Deng, Q.; Li, Y.; Chen, G.; Yan, J.; Zhang, J.; Meng, M.; Qu, C.; Jeje, A. Water-Soluble Complexes Catalyzed Coupling Aquathermolysis of Water-Heavy Oil-Methanol at Low Temperature. *Pet. Chem.* **2018**, *58*, 727–732. [[CrossRef](#)]
30. Clark, P.D.; Dowling, N.I.; Hyne, J.B.; Lesage, K.L. The Chemistry of Organosulphur Compound Types Occurring in Heavy Oils: 4. The High-Temperature Reaction of Thiophene and Tetrahydrothiophene with Aqueous Solutions of Aluminium and First-Row Transition-Metal Cations. *Fuel* **1987**, *66*, 1353–1357. [[CrossRef](#)]
31. Clark, P.D.; Dowling, N.I.; Lesage, K.L.; Hyne, J.B. Chemistry of Organosulphur Compound Types Occurring in Heavy Oil Sands: 5. Reaction of Thiophene and Tetrahydrothiophene with Aqueous Group VIIIIB Metal Species at High Temperature. *Fuel* **1987**, *66*, 1699–1702. [[CrossRef](#)]
32. Zhong, L.G.; Liu, Y.J.; Fan, H.F.; Jiang, S.J. Liaohe Extra-Heavy Crude Oil Underground Aquathermolytic Treatments Using Catalyst and Hydrogen Donors under Steam Injection Conditions. In Proceedings of the SPE international Improved Oil Recovery Conference in Asia Pacific, SPE, Kuala Lumpur, Malaysia, 20–21 October 2003; p. SPE-84863.
33. Hanyong, L.; Xin, L.; Daming, Z.; Guotao, Z.; Bo, Y. Preparation of Graphene Supported Ni-Fe Bimetallic Nanocatalyst and Its Catalytic Upgrading and Viscosity Reduction Performance for Heavy Oil. *Geoenergy Sci. Eng.* **2023**, *227*, 211847. [[CrossRef](#)]
34. Zhao, X.; Tan, X.; Liu, Y. Behaviors of Oil-Soluble Catalyst for Aquathermolysis of Heavy Oil. *Ind. Catal.* **2008**, *16*, 31.
35. Yusuf, A.; Al-Hajri, R.S.; Al-Waheibi, Y.M.; Jibril, B.Y. In-Situ Upgrading of Omani Heavy Oil with Catalyst and Hydrogen Donor. *J. Anal. Appl. Pyrolysis* **2016**, *121*, 102–112. [[CrossRef](#)]
36. Chen, Y.; Wang, Y.; Wu, C.; Xia, F. Laboratory Experiments and Field Tests of an Amphiphilic Metallic Chelate for Catalytic Aquathermolysis of Heavy Oil. *Energy Fuels* **2008**, *22*, 1502–1508. [[CrossRef](#)]
37. Dessouky, S.M.; Al-Sabagh, A.M.; Betiha, M.A.; Badawi, A. Catalytic Aquathermolysis of Egyptian Heavy Crude Oil. *Int. J. Chem. Mol. Nucl. Mater. Metall. Eng.* **2013**, *7*, 638–643.
38. Zhao, F.; Wang, X.; Wang, Y.; Shi, Y. The catalytic aquathermolysis of heavy oil in the presence of a hydrogen donor under reservoirs conditions. *J. Chem. Pharm. Res.* **2014**, *6*, 2037–2041.
39. Angeles, M.J.; Leyva, C.; Ancheyta, J.; Ramírez, S. A Review of Experimental Procedures for Heavy Oil Hydrocracking with Dispersed Catalyst. *Catal Today* **2014**, *220–222*, 274–294. [[CrossRef](#)]

40. Abdelsalam, Y.I.I.; Aliev, F.A.; Mirzayev, O.O.; Sitnov, S.A.; Katnov, V.E.; Akhmetzyanova, L.A.; Mukhamatdinova, R.E.; Vakhin, A.V. Aquathermolysis of Heavy Crude Oil: Comparison Study of the Performance of  $\text{Ni}(\text{CH}_3\text{COO})_2$  and  $\text{Zn}(\text{CH}_3\text{COO})_2$  Water-Soluble Catalysts. *Catalysts* **2023**, *13*, 873. [[CrossRef](#)]
41. Berezovskiy, D.A.; Kusov, G.V.; Shakmelikyan, M.G.; Cumbe, E.L.V. Analysis of Thermal Effects Technologies on Highly Viscous Oil Deposits of the Uzen Field. *Science. Eng. Technol. Polytech. Bull.* **2017**, *2*, 100–123.
42. *ASTM D86*; Standard Test Method for Distillation of Petroleum Products at Atmospheric Pressure. ASTM: West Conshohocken, PA, USA, 2014.
43. Li, X.; Chi, P.; Guo, X.; Sun, Q. Effects of Asphaltene Concentration and Asphaltene Agglomeration on Viscosity. *Fuel* **2019**, *255*, 115825. [[CrossRef](#)]
44. Sinha, U.; Dindoruk, B.; Soliman, M.Y. Development of a New Correlation to Determine Relative Viscosity of Heavy Oils with Varying Asphaltene Content and Temperature. *J. Pet. Sci. Eng.* **2019**, *173*, 1020–1030. [[CrossRef](#)]
45. Shabalin, K.V.; Foss, L.E.; Borisova, Y.Y.; Borisov, D.N.; Yakubova, S.G.; Yakubov, M.R. Study of the Heavy Oil Asphaltenes Oxidation Products Composition Using EPR and IR Spectroscopy. *Pet. Sci. Technol.* **2020**, *38*, 992–997. [[CrossRef](#)]
46. Rej, S.; Hejazi, S.M.H.; Badura, Z.; Zoppellaro, G.; Kalytchuk, S.; Kment, Š.; Fornasiero, P.; Naldoni, A. Light-Induced Defect Formation and Pt Single Atoms Synergistically Boost Photocatalytic  $\text{H}_2$  Production in 2D  $\text{TiO}_2$ -Bronze Nanosheets. *ACS Sustain. Chem. Eng.* **2022**, *10*, 17286–17296. [[CrossRef](#)]

**Disclaimer/Publisher’s Note:** The statements, opinions and data contained in all publications are solely those of the individual author(s) and contributor(s) and not of MDPI and/or the editor(s). MDPI and/or the editor(s) disclaim responsibility for any injury to people or property resulting from any ideas, methods, instructions or products referred to in the content.